Thermal expansion of $Li_3Na_3In_2F_{12}$ garnet

2006 J. Phys.: Condens. Matter 18 8925

(http://iopscience.iop.org/0953-8984/18/39/022)

INSTITUTE OF PHYSICS PUBLISHING JOURNAL OF PHYSICS: CONDENSED MATTER

J. Phys.: Condens. Matter **18** (2006) 8925–8934 doi:10.1088/0953-8984/18/39/022

Thermal expansion of $Li_3Na_3In_2F_{12}$ garnet

Andrzej Grzechnik[1,3], Hannes Krüger[2], Volker Kahlenberg[2] and Karen Friese[1]

[1] Departamento de Física de la Materia Condensada, Universidad del País Vasco, E-48080 Bilbao, Spain
[2] Institut für Mineralogie und Petrographie, Leopold-Franzens-Universität A-6020 Innsbruck, Austria

E-mail: andrzej@wm.lc.ehu.es

Received 29 June 2006, in final form 22 August 2006
Published 15 September 2006
Online at stacks.iop.org/JPhysCM/18/8925

Abstract

The structural behaviour of $Li_3Na_3In_2F_{12}$ garnet ($Ia\bar{3}d$, $Z = 8$) has been studied as a function of temperature (100 K $\leqslant T \leqslant$ 579 K) using single-crystal and powder x-ray diffraction at atmospheric conditions. The temperature dependence of the coefficient of thermal expansion is α (K^{-1}) $= 2.0 \times 10^{-5} + 2.4 \times 10^{-8}\ T$. The unit-cell volume change on cooling the $Li_3Na_3In_2F_{12}$ crystal from 298 to 100 K is equivalent to compressing it to about 0.5 GPa at room temperature. The effect of low temperature on the crystal structure is examined on the basis of structural parameters obtained from the refinements of the single-crystal data. The large coefficient of thermal expansion and the small bulk modulus of $Li_3Na_3In_2F_{12}$, in comparison with the oxide analogues, are due to massive changes in the In–F–Li interpolyhedral angle in the garnet framework at non-ambient conditions.

(Some figures in this article are in colour only in the electronic version)

1. Introduction

The crystal structure of $Li_3Na_3M_2F_{12}$ fluoride garnets ($Ia\bar{3}d$, $Z = 8$), where the M cations can be trivalent group III or transition metal ions (Al, Fe, Ga, In, Cr, etc), is a three-dimensional framework with each MF_6 octahedron joined to six others through vertex-sharing LiF_4 tetrahedra [1–6]. The Na^+ cations occupy eight-fold (triangulated dodecahedra or bisdisphenoids) interstitial positions (figure 1). Raman spectroscopy measurements indicate that $Li_3Na_3In_2F_{12}$ is stable down to at least 7 K at atmospheric conditions [7]. Machado *et al* [7] have also argued that anharmonic effects are not probable because of low thermal expansion of the $Li_3Na_3In_2F_{12}$ crystal and negligible temperature shifts of the observed Raman bands. On the other hand, a sudden drop in magnetic susceptibility occurring below about 75 and 30 mK

[3] Author to whom any correspondence should be addressed.

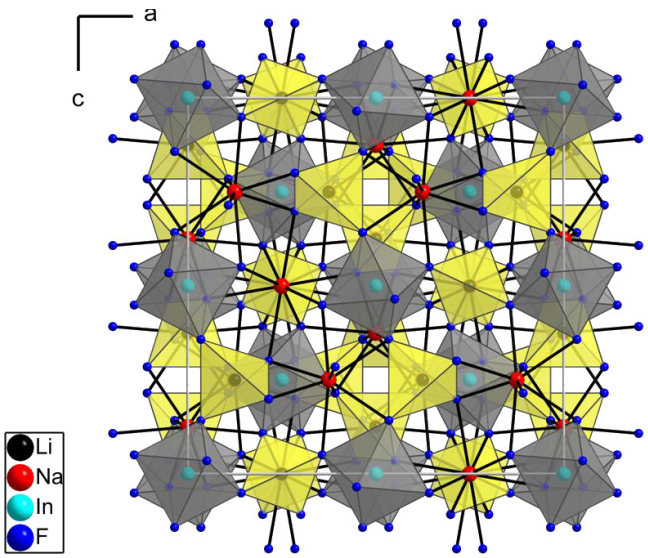

Figure 1. Crystal structure of $Li_3Na_3In_2F_{12}$ garnet ($Ia\bar{3}d$, $Z = 8$).

for $Li_3Na_3Fe_2F_{12}$ and $Li_3Na_3Cr_2F_{12}$, respectively, possibly suggests the existence of other low-temperature polymorphs [8].

The fluoride garnets $Li_3Na_3M_2F_{12}$ are of interest because of their luminescent properties for tunable lasers when doped with trivalent ions (mostly Cr^{3+}) in the octahedral sites [7, 9–15]. de Viry *et al* [9–11] have found that a radiative lifetime of the broad emission band between 700 and 1000 nm decreases when the temperature is raised from 10 to 300 K due to increasing phonon coupling with temperature. Based on theoretical calculations, Aramburu *et al* [15] have argued that some of the features in the spectra are rather charge-transfer bands, stronger than those due to the crystal-field processes. They have also modelled the sensitivity of the charge-transfer transitions to the variations in the Cr^{3+}–F^- distance. The *red*-shift of certain bands on warming the crystal from a few Kelvins to room temperature has been assigned to a lengthening of the Cr^{3+}–F^- distances induced by thermal expansion effects.

Our previous study on $Li_3Na_3In_2F_{12}$ garnet examined its high-pressure behaviour at room temperature [16]. It turns out that the bulk modulus is unusually small, $B_0 = 36.2(5)$ GPa. The reason why the trilithium trisodium diindium fluoride is so soft is a massive change of the Li–F–In angle between the LiF_4 tetrahedra and InF_6 octahedra (figure 1). The increasing distortions of the InF_6 octahedra that are the least compressible polyhedra in the structure explain the increase in the exponential lifetime of the $^4T_2$ emission in the Cr^{3+} luminescence spectra at high pressures [11]. The influence of external pressure on the distortions of the InF_6 octahedra in $Li_3Na_3In_2F_{12}$ corresponds to the M^{3+} ionic-radius effect on the distortion of the MF_6 octahedra in other $Li_3Na_3M_2F_{12}$ garnets at ambient conditions [16]. The crystalline field at the octahedral site could be changed by varying the M cations. When the M cations are large, the crystalline field is weak and Cr^{3+} luminescence spectra show a wide emission band [7, 11].

The aim of this study is to precisely determine thermal expansion of $Li_3Na_3In_2F_{12}$ garnet at atmospheric pressure. We are especially interested in finding out whether the effect of low temperature on the crystal structure of this garnet is equivalent to the effect of high pressure. Our structural results provide new data helpful in interpreting the optical and vibrational properties of this material [7, 15].

Table 1. Experimental details for single-crystal measurements.

Temperature (K)	250	200	150	100
Crystal data				
a (Å)	12.694(1)	12.675(1)	12.659(1)	12.648(1)
V (Å^3)	2045.5(5)	2036.3(5)	2028.6(5)	2023.3(5)
ρ (g cm^{-3})	3.554	3.570	3.584	3.593
μ (mm^{-1})	4.784	4.806	4.824	4.837
G_{iso}	0.09(5)	0.06(4)	0.06(4)	0.12(2)
Data collection [a]				
No. measured refl.	6338	6312	6294	6323
Range of hkl	$-16 \leqslant h \leqslant 16$	$-15 \leqslant h \leqslant 16$	$-15 \leqslant h \leqslant 16$	$-15 \leqslant h \leqslant 15$
	$-16 \leqslant k \leqslant 15$	$-16 \leqslant k \leqslant 15$	$-15 \leqslant k \leqslant 15$	$-15 \leqslant k \leqslant 14$
	$-15 \leqslant l \leqslant 15$	$-15 \leqslant l \leqslant 15$	$-15 \leqslant l \leqslant 15$	$-15 \leqslant l \leqslant 15$
No. unique refl.	181	182	180	181
No. observed refl.[b]	173	175	177	176
$R(\text{int})_{obs/all}$	3.06/3.11	3.37/3.41	3.32/3.33	3.57/3.59
sin $(\theta)/\lambda$	0.630 220	0.633 625	0.631 962	0.630 037
T_{min}/T_{max}	0.448/0.728	0.446/0.734	0.445/0.732	0.444/0.732
Refinement [c]				
R_{obs}	2.43	2.38	2.37	2.13
wR_{obs}	4.00	3.95	3.95	3.56
R_{all}	2.68	2.57	2.46	2.29
wR_{all}	4.10	4.04	3.97	3.62
GoF_{all}	2.87	2.90	2.89	2.59
GoF_{obs}	2.87	2.89	2.91	2.58
No. parameters	17	17	17	17

[a] Analytical absorption correction (crystal approximated by 23 faces).
[b] Criterion for observed reflections is $|F_{obs}| > 3\sigma$.
[c] All agreement factors are given in %, weighting scheme $1/[\sigma^2 (F_{obs}) + (0.01 F_{obs})^2]$.

2. Experimental details

The ambient-pressure room-temperature lattice parameter and unit-cell volume of $Li_3Na_3In_2F_{12}$ garnet studied here are $a_0 = 12.7070(14)$ Å and $V_0 = 2051.76(69)$ Å^3, respectively [16]. A polycrystalline sample of $Li_3Na_3In_2F_{12}$ was studied with x-ray powder diffraction at high temperatures on the Diff beamline at the ANKA Synchrotron Light Source in Karlsruhe and with a laboratory diffractometer. The measurement at 579 K in ANKA was carried out in the Bragg–Brentano geometry ($\lambda = 0.953\,45$ Å) with the angular step of 0.004°. The data were normalized with the monitor counting rates. The helium-purged heating chamber constructed by Physikalische Geräte GmbH Karlsruhe was used. The temperature was calibrated using the temperature dependence of the lattice parameter of silicon [17] mixed with the sample as an internal standard. The patterns at 373 and 423 K were recorded in the air with a Philips X-Pert MPD diffractometer (Cu Kα_1) equipped with an Anton Parr high temperature attachment. The sample was mounted on a platinum strip, which served as a sample holder as well as a heater. The XRD patterns were recorded with the angular step of 0.028°.

Diffraction intensities of a single crystal of $Li_3Na_3In_2F_{12}$ were measured with a Stoe IPDS II diffractometer (wavelength 0.710 73 Å) at different temperatures (250, 200, 150, and 100 K) using the Cryostream 700 N_2 cooling device (Oxford Cryosystems). More experimental details are given in table 1.

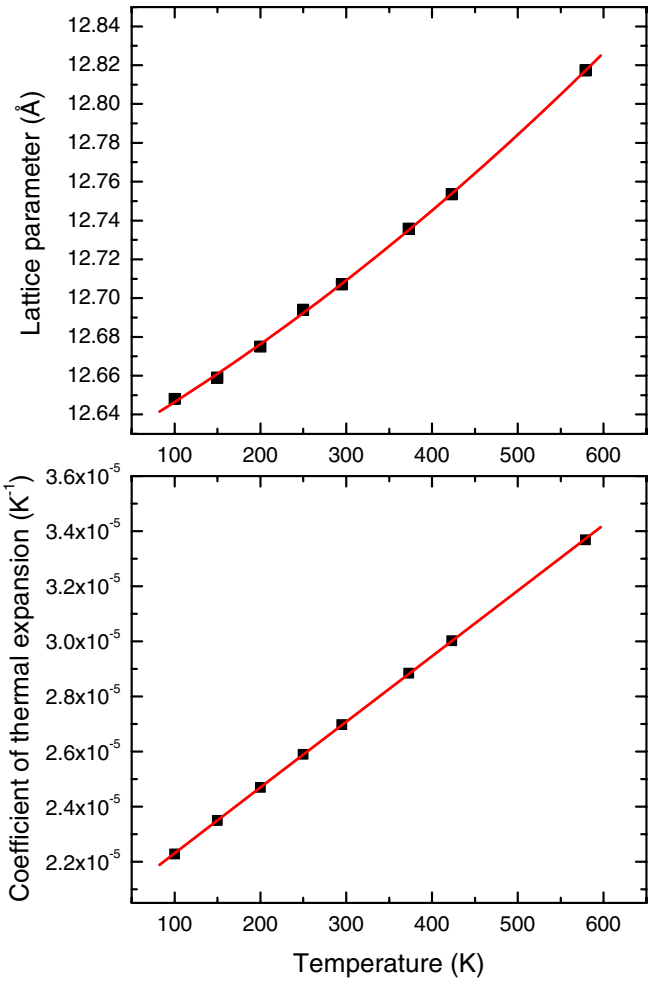

Figure 2. Temperature dependence of the lattice parameter and coefficient of thermal expansion.

3. Results

The temperature dependence of the lattice parameter and the coefficient of thermal expansion for $Li_3Na_3In_2F_{12}$ are shown in figure 2. The temperature dependence of the lattice parameter could be fitted with a polynomial function $a = 12.620 + 2.504 \times 10^{-4}\ T + 1.566 \times 10^{-7}\ T^2$. The linear thermal-expansion coefficient α is defined as $\alpha = (\mathrm{d}a/\mathrm{d}T)/a$ and could be fitted with a linear function $\alpha = 2.0 \times 10^{-5} + 2.4 \times 10^{-8}\ T$. This coefficient is $2.7 \times 10^{-5}\ \mathrm{K}^{-1}$ at $T = 298$ K.

More information on the evolution of the crystal structure at low temperatures has been extracted from the single-crystal measurements. The refinements of the data have been made with the program JANA2000 [18]. Structural parameters are given in tables 1–3.[4] The starting structural model for all the refinements has consisted of the In and Na atoms at Wyckoff positions 16a (0, 0, 0) and 24c (0.125, 0, 0.25), respectively [1, 16]. The positions of Li and

[4] Further details of the crystallographic investigations can be obtained from the Fachinformationszentrum Karslruhe, D-76344 Eggenstein-Leopoldshafen, Germany, on quoting the depository numbers CSD 416926-416929.

Table 2. Fluorine atomic positions from single-crystal refinements.

Temperature (K)	250	200	150	100
x	0.151 03(14)	0.151 09(13)	0.151 24(12)	0.151 31(12)
y	0.030 10(14)	0.030 14(13)	0.030 17(13)	0.030 17(12)
z	0.447 92(14)	0.447 58(13)	0.447 10(13)	0.446 82(12)

Table 3. Displacement parameters from single-crystal refinements.

	U_{11}	U_{22}	U_{33}	U_{12}	U_{13}	U_{23}	U_{iso}
250 K							
Li	—	—	—	—	—	—	0.016(2)
Na	0.015(1)	0.022(1)	U_{11}	0	0.003(1)	0	0.0199(6)
In	0.0125(4)	U_{11}	U_{11}	−0.0005(1)	U_{12}	U_{12}	0.0125(3)
F	0.013(1)	0.021(1)	0.020(1)	−0.0025(7)	0.001(1)	−0.0005(7)	0.0181(6)
200 K							
Li	—	—	—	—	—	—	0.015(2)
Na	0.013(1)	0.018(1)	U_{11}	0	0.002(1)	0	0.0165(6)
In	0.0109(4)	U_{11}	U_{11}	−0.0004(1)	U_{12}	U_{12}	0.0109(2)
F	0.011(1)	0.018(1)	0.017(1)	−0.0014(7)	0.0028(7)	−0.006(6)	0.0152(5)
150 K							
Li	—	—	—	—	—	—	0.012(2)
Na	0.011(1)	0.015(1)	U_{11}	0	0.0012(1)	0	0.0138(6)
In	0.0094(4)	U_{11}	U_{11}	−0.0003(1)	U_{12}	U_{12}	0.0094(2)
F	0.009(1)	0.016(1)	0.014(1)	−0.0010(7)	0.0023(7)	−0.0002(6)	0.0127(5)
100 K							
Li	—	—	—	—	—	—	0.012(2)
Na	0.009(1)	0.0116(8)	U_{11}	0	0.0003(8)	0	0.0108(5)
In	0.0079(4)	U_{11}	U_{11}	−0.0002(1)	U_{12}	U_{12}	0.0079(2)
F	0.0076(8)	0.0132(8)	0.0113(8)	0.0005(6)	−0.0023(6)	0.0002(6)	0.0107(5)

F atoms have been determined from the difference F_{obs}–F_{calc} Fourier synthesis. The Li atom is at the Wyckoff position 24d (0.375, 0, 0.25), while the F atom is located at the Wyckoff site 96 h (x, y, z) (table 2). Except for Li, the displacement parameters for Na, In, and F have been refined anisotropically (table 3). An isotropic Gaussian extinction correction (G_{iso}) has also been applied [19] (table 1).

In similar studies to this one here, structural parameters are generally plotted as a function of temperature. As in this case we are interested in comparing the effects of temperature and pressure on the crystal structure, we would rather plot the structural parameters as a function of a unit-cell volume normalized to the unit-cell volume at room temperature and atmospheric pressure, $V_0 = 2051.76(69)$ Å^3. This allows for a direct comparison of the structural changes on cooling and on compression; e.g., expansivities and compressibilities of polyhedral volumes could be compared. The volume change on cooling from 298 to 100 K at atmospheric pressure (table 1) corresponds to compressing the $Li_3Na_3In_2F_{12}$ material to about 0.5 GPa at room temperature, according to the equation of state reported earlier [16]. Figure 3 shows the dependences of normalized polyhedral volumes [20], bond distances, and In–F–Li angles on the reduced unit-cell volume. The NaF_8 triangulated dodecahedra are the most sensitive to the change of the unit-cell volume. The bonds between the fluorine atoms and the nearest-neighbour cations have the same behaviour at high pressures and low temperatures. The In–F, Li–F, and Na–F(2) bonds are nearly constant, while the two Na–F bonds have a tendency to become equal at the reduced unit-cell volume of $V/V_0 = 0.88$. Unlike at high pressures, the

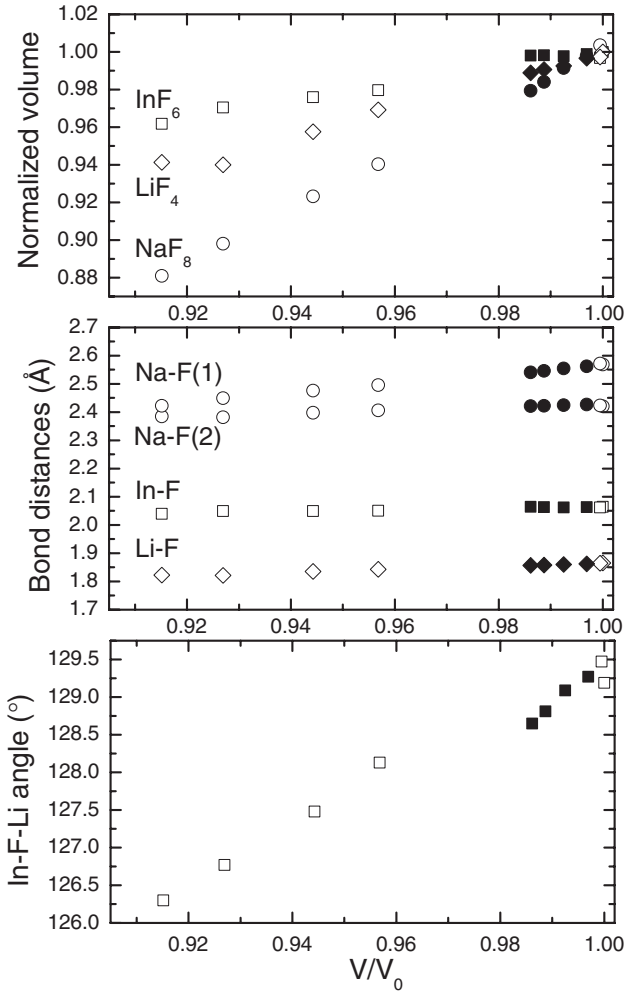

Figure 3. Dependence of the normalized polyhedral volumes, bond distances, and In–F–Li angles on the reduced unit-cell volume. Open and full symbols represent the high-pressure [16] and low-temperature (this study) data, respectively.

volume of the InF_6 octahedra is constant when the temperature is lowered. The temperature-induced changes in the In–F–Li angle between the InF_6 and LiF_4 polyhedra that constitute the three-dimensional structure of $Li_3Na_3In_2F_{12}$ garnet are relatively larger than the pressure-induced ones (see the slopes for the data points obtained at low temperatures and high pressures, respectively). Our data shown in figure 3 suggest that the sensitivity of the In–F–Li angle to temperature results in a relatively high coefficient of thermal expansion of $Li_3Na_3In_2F_{12}$.

The parameters to estimate the polyhedral distortions expressed as relative changes (all in %) of the angles in the LiF_4 tetrahedra, Na–F bonds in the NaF_8 triangulated dodecahedra, F–F distances and F–In–F angles in the InF_6 octahedra[5] are also plotted as a function of the reduced

[5] The bond-length distortion of the NaF_8 triangulated dodecahedra is $100|d_1–d_2|/|d_1+d_2|$, where d_1 and d_2 are Na–F distances. The edge-length distortion of the InF_6 octahedra is $100|f_1–f_2|/|f_1+f_2|$, where f_1 and f_2 are F–F distances in the octahedra. The angular distortion of the LiF_4 tetrahedra is $100\ (|\alpha_1-\alpha_0|+2|\alpha_2-\alpha_0|)/(3\alpha_0)$, where α_1 and α_2 are tetrahedral angles, while $\alpha_0 = 109.471°$. The angular distortion of the InF_6 octahedra is $100|\beta_1-\beta_2|/90$, where β_1 and β_2 are octahedral angles.

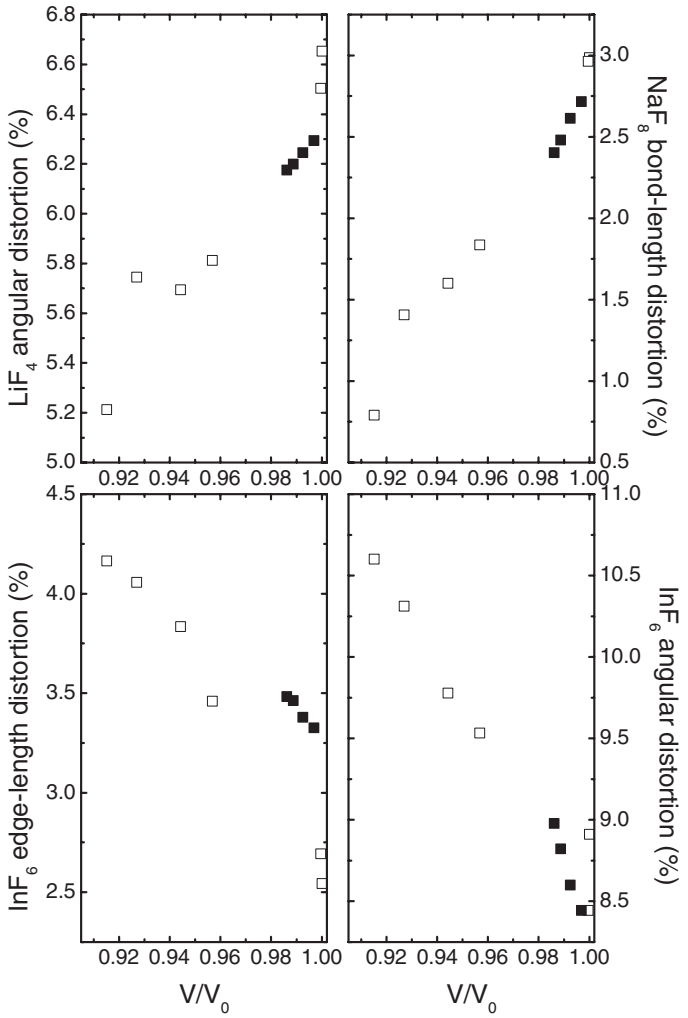

Figure 4. Dependence of angular, bond-length, and edge-length distortions in LiF_4, InF_6, and NaF_8 polyhedra on the reduced unit-cell volume. Open and full symbols represent the high-pressure [16] and low-temperature (this study) data, respectively.

unit-cell volume in figure 4. Our data clearly demonstrate that the LiF_4 tetrahedra become more regular, while the bond-length distortion of the NaF_8 polyhedra diminishes because the two independent Na–F distances tend to converge at $V/V_0 = 0.88$ (figure 3). Both distortion parameters for the InF_6 octahedra increase on cooling and compression. However, the InF_6 angular distortion is more sensitive to temperature than to pressure.

The mean-square displacement amplitude $\langle|U_j^2|\rangle$ of the atom j is expected to change linearly as a function of temperature and extrapolate to zero at $T = 0$ K [21–23]. A deviation from the linear behaviour might be due to static disorder, zero-point motion, or due to anharmonic vibrations of the atoms at high temperatures. The linear fit to the data and their extrapolation to $T = 0$ K are usually disturbed by too few data points and possible correlations of the displacement amplitudes with other variables in the structure refinement, e.g., the scale factor or an extinction coefficient. An analysis of the data in table 3 shows that the intercepts at

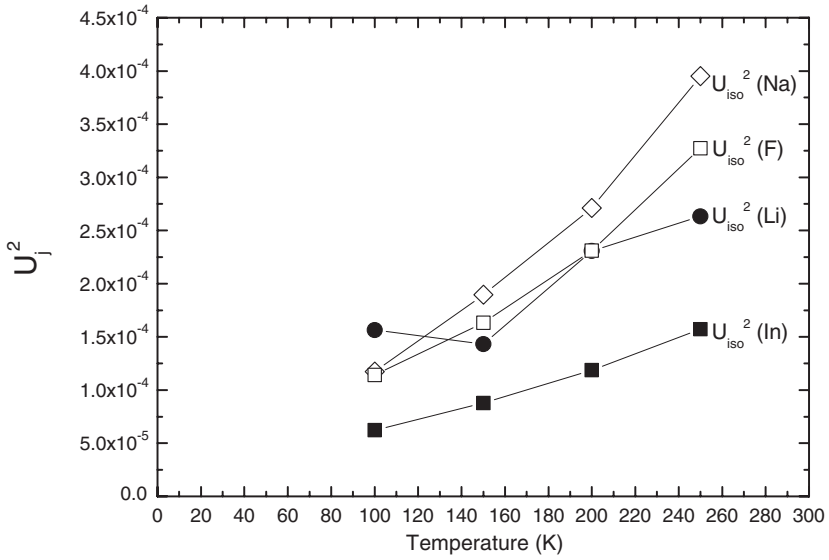

Figure 5. Temperature dependence of mean-square displacement amplitudes $U^2_{\rm iso}$ for the Li, Na, In, and F atoms.

$T = 0$ K resulting from the interpolation of the cationic mean-square displacement amplitudes are not significant for the In^{3+}, Na^+, and F^- ions (figure 5). The unexpectedly larger $U_{\rm iso}$ amplitude for the Li^+ ion at 100 K might be an indication of a static disorder of the Li^+ ions[6].

4. Discussion

The results of our study show that the coefficient of thermal expansion in $Li_3Na_3In_2F_{12}$ ($Ia\bar{3}d$, $Z = 8$) is $\alpha = 2.7 \times 10^{-5}$ K^{-1} at $T = 298$ K. Table 4 compares this value with the thermal coefficients at room temperature for several oxide garnets recalculated from the experimental data reported in the literature. The α parameter for $Li_3Na_3In_2F_{12}$ is larger than for any of the oxide garnets. In fact, it is higher than the parameters for the silicate garnets ($Mn_3Al_2Si_3O_{12}$, $Ca_3Al_2Si_3O_{12}$, and $Mg_3Al_2Si_3O_{12}$) by a factor of about five. This observation correlates very well with the fact that the bulk modulus of $Li_3Na_3In_2F_{12}$ is one order of magnitude lower than the moduli of silicate garnets [16]. Our data suggest that such a behaviour is due to large changes in the In–F–Li interpolyhedral angle in the garnet framework on cooling and compression.

The results presented here could help to understand the luminescent properties of $Li_3Na_3In_2F_{12}$ at various pressure and temperature conditions. The unit-cell volume change on cooling the $Li_3Na_3In_2F_{12}$ crystal from 298 to 100 K is equivalent to compressing it to about 0.5 GPa at room temperature. Hence, it still needs to be clarified whether the effects of pressure and temperature on the optical properties could also be equivalent [7, 9–15], since some of the structural features respond differently to pressures and temperatures. The fact that

[6] A refinement of the anisotropic displacement parameters of Li provides no further information of underlying static disorder. Although this refinement leads to reasonable values it was discarded by us, as we considered an anisotropic refinement of this very light atom to be exaggerated. A close inspection of the electron density around the Li-atom position also gave no clear indication of disorder. We therefore assume that the non-ideal behaviour of the displacement parameters of Li might also be attributed to small systematic errors in the experimental data, e.g. insufficient correction for extinction [24].

Table 4. Coefficients of thermal expansion for $Li_3Na_3In_2F_{12}$ and oxide garnets at $T = 298$ K.

Material	α (K^{-1})	Reference
$Li_3Na_3In_2F_{12}$	2.7×10^{-5}	This study
$Mn_3Al_2Si_3O_{12}$	5.3×10^{-6}	[21]
$Ca_3Al_2Si_3O_{12}$	5.4×10^{-6}	[21]
$Mg_3Al_2Si_3O_{12}$	7.5×10^{-6}	[22]
$Y_3Fe_2Fe_3O_{12}$	1.1×10^{-5}	[25]
$Gd_3Ga_2Ga_3O_{12}$	7.8×10^{-6}	[25]
$Gd_3Fe_2Fe_3O_{12}$	1.0×10^{-5}	[25]
$Y_3Al_2Al_3O_3$	7.7×10^{-6}	[25]
$Y_3Ga_2Ga_3O_{12}$	7.5×10^{-6}	[25]
$Y_3Al_5O_{12}$	6.8×10^{-6}	[26]

the In–F bond distances (or Cr–F distances when the material is doped) and InF_6 polyhedral volumes hardly (if at all) change on cooling implies that the sensitivity of the charge-transfer transitions to the variations of the Cr–F distance, discussed by Aramburu *et al* [15], ought to be investigated in more detail. Here, we demonstrate that the most sensitive structural features to temperature are in fact the angular distortions of the InF_6 octahedra that influence the crystal field [7, 11, 16]. The temperature dependence of the coefficient α shown in figure 2, instead of $\alpha = 2 \times 10^{-5}$ K^{-1} [15], is useful for the calculations of the changes in charge-transfer energies due to the thermal expansion. It should also be helpful to further characterize the thermo-optic effects [25, 26] in this garnet material.

5. Conclusions

The coefficient of thermal expansion in $Li_3Na_3In_2F_{12}$ ($Ia\bar{3}d$, $Z = 8$), $\alpha = 2.7 \times 10^{-5}$ K^{-1} at $T = 298$ K, is higher than the coefficients for oxide garnets. The volume change from 298 to 100 K at atmospheric pressure corresponds to compressing the $Li_3Na_3In_2F_{12}$ material to about 0.5 GPa at room temperature. The effects of pressure and temperature result in a massive change of the In–F–Li angle between the InF_6 octahedra and LiF_4 tetrahedra in the three-dimensional structure (figures 1 and 2). Unlike on compression, the volume of the InF_6 octahedra practically does not change on cooling. The angular InF_6 distortion is more sensitive to temperature than to pressure.

Acknowledgments

This work was supported by a bilateral action of the Austrian Exchange Service (ÖAD) and the Spanish Ministerio de Ciencia y Tecnología (Programa Acciónes Integradas). The synchrotron experiment at the ANKA Synchrotron Light Source in Karlsruhe was supported by the European Community—Research Infrastructure Action under FP6: Structuring the European Research Area, Integrating Activity on Synchrotron and Free Electron Laser Science (IA-SFS, RII3-CT-2004-506008). We thank S Doyle for his technical assistance at ANKA. AG and KF acknowledge additional financial support from the Ministerio de Ciencia y Tecnología and the Gobierno Vasco.

References

[1] de Pape R, Portier J, Grannec J, Gauthier G and Hagenmuller P 1969 *C. R. Acad. Sci., Paris* C **269** 1120
[2] Geller S 1971 *Am. Mineral.* **56** 18

[3] Morell A, Tanguy B, Portier J and Hagenmuller P 1974 *J. Fluorine Chem.* **3** 351
[4] Tekeda Y, Sone M, Suwa Y, Inagaki M and Naka S 1977 *J. Solid State Chem.* **20** 261
[5] Langley R H and Sturgeon G D 1979 *J. Fluorine Chem.* **14** 1
[6] Massa W, Post B and Babel D 1982 *Z. Kristallogr.* **158** 299
[7] Machado M A C, Pachoal C W A, Mendes Filho J, Ayala A P, Moreira R L and Gesland J-Y 2002 *J. Phys.: Condens. Matter* **14** 271
[8] Chamberlain S and Corruccini L R 1997 *J. Phys. Chem. Solids* **58** 899
[9] de Viry D, Denis J P, Blanzat B and Grannec J 1987 *J. Solid State Chem.* **71** 109
[10] de Viry D, Pellé F, Denis J P, Blanzat B, Grannec J and Chaminade J P 1987 *J. Fluorine Chem.* **35** 244
[11] de Viry D, Denis J P, Tercier N and Blanzat B 1987 *Solid State Commun.* **63** 1183
[12] Caird J A, Payne S A, Staver P R, Ramponi A J, Chase L L and Krupke W F 1988 *IEEE J. Quantum Electron.* **24** 1077
[13] de Viry D, Casalboni M and Palumno M 1990 *Solid State Commun.* **76** 1051
[14] de Viry D, Pilla O, Pellé F and Blanzat B 1991 *J. Lumin.* **48/49** 561
[15] Aramburu J A, Barriuso M T and Moreno M 1996 *J. Phys.: Condens. Matter* **8** 6901
[16] Grzechnik A, Balic-Zunic T, Makovicky E, Gesland J-Y and Friese K 2006 *J. Phys.: Condens. Matter* **18** 2915
[17] Okada Y and Tokumaru Y 1984 *J. Appl. Phys.* **56** 314
[18] Petricek V, Dusek M and Palatinus L 2000 *Jana2000, The Crystallographic Computing System* (Praha: Institute of Physics)
[19] Becker P J and Coppens P 1974 *Acta Crystallogr.* A **30** 129
[20] Balic-Zunic T and Vickovic I 1996 *J. Appl. Crystallogr.* **29** 305
[21] Dove M T 1993 *Introduction to Lattice Dynamics* (Cambridge: Cambridge University Press)
[22] Rodehorst U, Geiger C A and Armbruster T 2002 *Am. Mineral.* **87** 542
[23] Pavese A, Artioli G and Prencipe M 1995 *Am. Mineral.* **80** 457
[24] Giacovazzo C (ed) 2002 *Fundamentals of Crystallography* 2nd edn (Oxford: Oxford University Press)
[25] Geller S, Espinosa G P and Crandall P B 1969 *J. Appl. Crystallogr.* **2** 86
[26] Wynne R, Daneu J L and Fan T Y 1999 *Appl. Opt.* **38** 3282